Modulation of pulsatile GnRH dynamics across the ovarian cycle: the role of glutamatergic transmission in the arcuate kisspeptin network.

Margaritis Voliotis[1,*,†] , Xiao Feng Li[2,†], Ross De Burgh[2,†], Geffen Lass[2], Deyana Ivanova[2], Caitlin McIntyre[2],Kevin T. O'Byrne[2,*], Krasimira Tsaneva-Atanasova[1,*]
[1] Department of Mathematics and Living Systems Institute, College of Engineering, Mathematics and Physical Sciences, University of Exeter, Exeter, EX4 4QF, UK.
[2] Department of Women and Children's Health, School of Life Course Sciences, King's College London, London SE1 1UL, UK.
[†] These authors contributed equally to this work
[*] For correspondence: M.Voliotis@exeter.ac.uk, Kevin.O'Byrne@kcl.ac.uk, K.Tsaneva-Atanasova@exeter.ac.uk

Abstract

Pulsatile GnRH release is essential for normal reproductive function. Kisspeptin secreting neurons found in the arcuate nucleus, known as KNDy neurons for co-expressing neurokinin B, and dynorphin, drive pulsatile GnRH release. Furthermore, gonadal steroids regulate GnRH pulsatile dynamics across the ovarian cycle by altering KNDy neurons' signalling properties. However, the precise mechanism of regulation remains mostly unknown. To better understand these mechanisms we start by perturbing the KNDy system at different stages of the estrous cycle using optogenetics. We find that optogenetic stimulation of KNDy neurons stimulates pulsatile GnRH/LH secretion in estrous mice but inhibits it in diestrous mice. These in-vivo results in combination with mathematical modelling suggest that the transition between estrus and diestrus is underpinned by well-orchestrated changes in neuropeptide signalling and in the excitability of the KNDy population controlled via glutamate signalling. Guided by model predictions, we show that blocking glutamate signalling in diestrous animals inhibits LH pulses, and that optic stimulation of the KNDy population mitigates this inhibition. In estrous mice, disruption of glutamate signalling inhibits pulses generated via sustained low-frequency optic stimulation of the KNDy population, supporting the idea that the level of network excitability is critical for pulse

generation. Our results reconcile previous puzzling findings regarding the estradiol-dependent effect that several neuromodulators have on the GnRH pulse generator dynamics. Therefore, we anticipate our model to be a cornerstone for a more quantitative understanding of the pathways via which gonadal steroids regulate GnRH pulse generator dynamics. Finally, our results could inform useful repurposing of drugs targeting the glutamate system in reproductive therapy.

Introduction

The dynamics of gonadotropin-releasing hormone (GnRH) secretion is critical for reproductive health. In female animals, GnRH secretion is tightly regulated across the ovarian cycle. Pulsatile secretion dominates most of the cycle, with frequency and amplitude modulated by the ovarian steroid feedback. Positive feedback from increasing estradiol levels triggers a preovulatory surge of GnRH/LH secretion (Christian and Moenter, 2010). Furthermore, there is ample evidence that ARC kisspeptin neurons are prime mediators of the ovarian steroid feedback on the pulsatile dynamics of GnRH/LH secretion (McQuillan et al., 2019), although the mechanisms remain unclear.

In-vitro studies have shown that gonadal steroids have a dramatic effect on the electrophysiology of ARC kisspeptin neurons. For instance, spontaneous firing activity of ARC kisspeptin neurons from castrated mice appears elevated compared to intact animals (Ruka et al., 2016) and estradiol replacement attenuates ARC kisspeptin neuron activity in gonadectomised animals (Ruka et al., 2016; Wang et al., 2018). More recently, fiber photometry data from female mice show that the ARC kisspeptin neuronal population (KNDy network) pulses at a relatively constant frequency throughout the ovarian cycle apart from the estrous phase where the frequency is dramatically reduced (McQuillan et al., 2019). This silencing effect is thought to be a direct consequence of the increasing progesterone levels in the circulation associated with ovulation (McQuillan et al., 2019). Furthermore, studies in the sheep indicate the silencing effect of progesterone is mediated through increased dynorphin signalling (Goodman et al., 2011; Moore et al., 2018), however this is less clear in mice where ovarian steroids have a negative effect on Dyn mRNA levels (Navarro et al., 2009).

Perplexing is also the differential effect of various neuromodulators on LH secretion depending on the gonadal steroid background. For instance, N-methyl-D-aspartate (NMDA) robustly inhibits LH pulses in the ovariectomized monkey whereas in the presence of

estradiol this effect is reversed, and NMDA stimulates LH secretion (Reyes et al., 1990; Reyes et al., 1991). Similar reversal of action on LH dynamics depending on the underlying ovarian steroid milieu has been also documented for other neurotransmitter and neuropeptides in other species (Kalra and Kalra, 1983; Brann and Mahesh, 1992; Arias et al., 1993; Bonavera et al., 1994; Scorticati et al., 2004) and highlights the complex mechanisms underlying the modulation the GnRH pulse generator by gonadal steroids.

Here, using mathematical modelling along with optogenetic stimulation of ARC kisspeptin neurons we embark to understand how the dynamics of the pulse generator are modulated across the ovarian cycle. Our mathematical model suggests that the level of excitability within the ARC kisspeptin network—the propensity of kisspeptin neurons to signal and activate each other—is one of the key parameters modulated in different stages of the cycle by gonadal steroids. Previous studies have shown that ARC kisspeptin neurons synapse on each other (Yip et al., 2015; Qiu et al., 2016) and are glutamatergic (Cravo et al., 2011; Qiu et al., 2011; Kelly et al., 2013; Nestor et al., 2016; Qiu et al., 2016; Wang et al., 2018). Based on these findings we hypothesise that population excitability should be enabled primarily via glutamate signalling. We test our predictions *in-vivo* and show that glutamatergic transmission is an important factor for the pulsatile behaviour of the KNDy network.

Materials and methods

Animals

Adult Kiss-Cre heterozygous transgenic female mice aged between 8-14 weeks, 25-30 g, were used for experiments (Yeo et al., 2016). Breeding pairs were obtained from the Department of Physiology, Development and Neuroscience, University of Cambridge, UK and mated in house at King's College London. Genotyping was performed using a multiplex PCR protocol for detection of heterozygosity for the Kiss-Cre or wild-type allele as previously described (Lass et al., 2020). Only mice with normal estrous cycles were used. Daily vaginal smears were performed for the detection of the estrous and diestrous stages of the ovarian cycle. Mice were singularly housed and provided with food (standard maintenance diet; Special Dietary Services, Wittam, UK) and water ad libitum while being kept under a 12:12 h light/dark cycle (lights on 0700 h) at 23 ± 2°C. All animal procedures performed were approved by the Animal Welfare and Ethical Review Body Committee at King’s College London and conducted in accordance with the UK Home Office Regulations.

Surgical procedures

Stereotaxic injection of AAV9-EF1-dflox-hChR2-(H134R)-mCherry-WPRE-hGH (4.35 x 10^{13} GC/ml; Penn Vector Core; University of Pennsylvania, PA, USA) for targeted expression of channelrhodopsin (ChR2) in ARC kisspeptin neurons was done under aseptic conditions. The mice were anaesthetised using ketamine (Vetalar, 100 mg/kg, i.p.; Pfizer, New York City, NY, USA) and xylazine (Rompun, 10 mg/kg, i.p.; Bayer, Leverkusen, Germany). Kiss-Cre female mice (n = 12) or wilt-type (n = 3) were secured in a Kopf Instruments motorized stereotaxic frame (Kopf Instruments, Tujunga, CA, USA) and surgical procedures on the brain were performed using a Robot Stereotaxy system (Neurostar, Tubingen, Germany). Stereotaxic injection coordinates used to target the ARC were obtained from the mouse brain atlas of Paxinos and Franklin (Paxinos and Franklin, 2004) (0.25 mm lateral, 1.94 mm posterior to bregma and at a depth of 5.8 mm). A skin incision was made and a small hole was drilled in the skull above the location of the ARC. A 2-µl Hamilton micro-syringe (Esslab, Essex, UK) was attached to the robot stereotaxy and used to inject 0.3µl of the AAV-construct into the ARC, unilaterally, at a rate of 100 nl/min. After the injection, the needle was left in position for 5 min and then slowly lifted over 1 min. The same coordinates as the injection site were then used to insert a fiber-optic cannula (200 µm, 0.39 NA, 1.25 mm ceramic ferrule; Thorlabs, LTD, Ely, UK), however a depth of 5.78 mm was reached to ensure the fiber-optic cannula was situated immediately above the injection site. Additionally, an intracerebroventricular (ICV) fluid guide cannulae (26 gauge; Plastics One) targeting the lateral ventricle (coordinates: 1.1 mm lateral, 1.0 mm posterior to bregma and at a depth of 3.0 mm) was chronically implanted. Dental cement (Superbond C&B kit Prestige Dental Products, Bradford UK) was used to fix the cannulae in place and the skin incision was sutured. A one week recovery period was given post-surgery. After this period, the mice were handled daily to acclimatize them to the tail-tip blood sampling procedure (Steyn et al., 2013). Mice were left for 4 weeks to achieve effective opsin expression before experimentation.

Validation of AAV injection site and fibre optic and ICV cannula position

Once experiments were completed, mice were given a lethal dose of ketamine and transcardially perfused for 5 min with heparinized saline, followed by 10 min of ice-cold 4% paraformaldehyde (PFA) in phosphate buffer, pH 7.4, for 15 min using a pump (Minipuls; Gilson). Brains were collected immediately and post fixed at 4°C in 15% sucrose in 4% PFA and left to sink. They were then transferred to 30% sucrose in PBS until they sank. The brains

were then snap-frozen on dry ice and stored at -80°C. Using a cryostat, every third coronal brain section (30 µm) was collected between -1.34 mm to -2.70 mm from bregma and sections were mounted on microscope slides, left to air-dry and cover slipped with ProLong Antifade mounting medium (Molecular Probes, Inc, OR, USA). Verification and evaluation of the injection site was performed using an Axioskop 2 Plus microscope equipped with axiovision 4.7 (Zeiss). One of 12 Kiss-Cre mice failed to show mCherry fluorescence in the ARC and was excluded from the analysis.

Experimental design and blood sampling for LH measurement.

For measurement of LH pulsatility during optogenetic stimulation, the tip of the mouse's tail was removed with a sterile scalpel for tail-tip blood sampling (Czieselsky et al., 2016). The chronically implanted fiber-optic cannula was attached to a multimode fiber-optic rotary joint patch cables (Thorlabs) via a ceramic mating sleeve. This allows for freedom of movement and blue light delivery (473 nm wavelength) using a Grass SD9B stimulator controlled DPSS laser (Laserglow Technologies) during optogenetic stimulation.

The experimental protocol involved an hour long acclimatisation period, followed by 2.5 h of blood sampling, where 5 µl of blood was collected every 5 min. For estrous and diestrous mice, optic stimulation was initiated after 1 h of control blood sampling and was sustained for 1.5 h h. Optic stimulation was delivered as 5ms pulses of light at 5 Hz with the laser intensity measured at the tip of the fiber-optic patch cable set to 5mW (Voliotis et al., 2019). Additionally, in separate experiments, diestrous mice were optically stimulated at 5 or 15 Hz for 2.5 h, that is entire blood sampling period. Control mice (in estrus or diestrus) received no optic stimulation. Wild-type mice (estrus and disetrus) received 5 Hz optic stimulation to verify that our optic stimulation protocol had no undesirable effects on LH secretion.

Neuropharmacological manipulation of glutamatergic signalling was performed using a combination of NMDA (AP5, Tocris, Abingdon, UK) and AMPA (CNQX, Alpha Aesar, Heysham, UK) receptor antagonist treatment with or without simultaneous optogenetic stimulation. The animals were prepared for optogenetic experimentation as described above with additional preparation of the ICV injection cannula. Immediately after connection of the fiber-optic cannula, the ICV injection cannula with extension tubing, preloaded with drug solution (AP5 and CNQX dissolved in artificial CSF) or artificial CSF alone as control, was inserted into the guide cannula. The extension tubing, reaching outside of the cage, was connected to a 10 µl Hamilton syringe mounted in an automated pump (Harvard Apparatus) to allow for remote micro-infusion without disturbing the animals during experimentation.

After a 55 min control blood sampling period, as described above, and 5 min before the onset of optic stimulation, a bolus ICV injection of drug solution (12 nmol AP5 and 5 nmol CNQX in 2.3 μl) was given over 5 min, followed by a continuous infusion (20 nmol AP5 and 10 nmol CNQX in 5.6 μl) for the remaining 90 min of experimentation. Artificial CSF controls, with or without optic stimulation, received the same ICV fluid regime. When no optic stimulation was applied the same ICV administration and blood sampling regimen described was applied. Stimulation and non-stimulation protocols were implemented in random order for Kiss-Cre mice.

The blood samples were snap-frozen on dry ice and stored at -80°C until processed. In-house LH enzyme-linked immunosorbent assay (LH ELISA) similar to that described by Steyn et al. was used for processing of the mouse blood samples (Steyn et al., 2013). The mouse LH standard (AFP- 5306A; NIDDK-NHPP) was purchased from Harbor-UCLA along with the primary antibody (polyclonal antibody, rabbit LH antiserum, AFP240580Rb; NIDDK-NHPP). The secondary antibody (donkey anti-rabbit IgG polyclonal antibody [horseradish peroxidase]; NA934) was from VWR International. Validation of the LH ELISA was done in accordance with the procedure described in Steyn et al. (Steyn et al., 2013) derived from protocols defined by the International Union of Pure and Applied Chemistry. Serially diluted mLH standard replicates were used to determine the linear detection range. Nonlinear regression analysis was performed using serially diluted mLH standards of known concentration to create a standard curve for interpolate the LH concentration in whole blood samples, as described previously (Voliotis et al., 2019). The intraassay and interassay variations were 4.6% and 10.2%, respectively.

LH pulse detection and statistical analysis.

Dynpeak algorithm was used for the detection of LH pulses (Vidal et al., 2012). The differential effect of optogenetic stimulation on LH pulsatility in estrus and diestrus was determined by looking at the frequency of LH pulses. For mice in estrus and for the neuropharmacological experiments, the mean ± SEM of LH pulses per hour were compared between the 60 min pre-stimulation/drug delivery control period and subsequent 90 min stimulation period. For mice in diestrus, the mean ± SEM of LH pulses per hour were compared between controls, 5 Hz and 15 Hz treatment groups, as optic stimulation was applied from the beginning of blood sample period. No optic stimulation was applied to control animals, however the same time points were compared. The frequency of LH pulses in the 90-min optic stimulation/drug delivery period was also compared between treatment

groups. One-way ANOVA followed by Dunnett's test, $p < 0.05$, was used to determine statistical significance.

Mathematical model of the KNDy network.

We used a modified version of our previously published mathematical model of the KNDy network (Voliotis et al., 2019). Briefly, the model describes the ARC kisspeptin population in terms of three variables: $\bar{D}$, the average concentration of Dyn secreted by the population; $\bar{N}$, the average concentration of NKB secreted by the population; and $\bar{v}$, the average firing activity of the population, measured in spikes/min. The variables obey the following set of coupled ordinary differential equations (ODEs):

$$\frac{d\bar{D}}{dt} = f_D(\bar{v}) - d_D\bar{D}; \quad [1]$$

$$\frac{d\bar{N}}{dt} = f_N(\bar{v}, \bar{D}) - d_N\bar{N}; \quad [2]$$

$$\frac{d\bar{v}}{dt} = f_v(\bar{v}, \bar{N}) - d_v\bar{v}. \quad [3]$$

Parameters d_D, d_N and d_v control the characteristic timescale of each variable. The secretion rate of Dyn and NKB are given by:

$$f_D(\bar{v}) = k_{D,0}\frac{\bar{v}^{n_1}}{\bar{v}^{n_1} + K_{v,1}^{n_1}};$$

$$f_N(\bar{v}, \bar{D}) = k_N\frac{\bar{v}^{n_2}}{\bar{v}^{n_2} + K_{v,2}^{n_2}}\frac{K_D^{n_3}}{\bar{D}^{n_3} + K_D^{n_3}}.$$

In the equations above neuronal activity ($\bar{v}$) stimulates secretion of both neuropeptides, and Dyn represses NKB secretion. The maximum secretion rate for the two neuropeptides is controlled by parameters k_D and k_N and we refer to these parameters as the strength of Dyn and NKB singalling respectively. The effector levels at which saturation occurs are controlled via parameters $K_{v,1}$, $K_{v,2}$ and K_D. Here, we are interested in investigating the effect of network excitability on the dynamics therefore we modify the equation for the neuronal activity, $\bar{v}$, by setting:

$$f_v(\bar{v}, \bar{N}) = v_0\frac{1-\exp(-I)}{1+\exp(-I)}; I = I_0 + k_v\left(\frac{N^{n_4}}{N^{n_4}+K_N^{n_4}}\bar{v}\right),$$

where we have introduced parameter k_v capturing the strength of the synaptic connections between KNDy neurons in the ARC and which we will use as a proxy for intrinsic network excitability. Furthermore, v_0 is the maximum rate at which the firing rate increases in

response to synaptic inputs I. Note the stimulatory effect of NKB (which is secreted at the presynaptic terminal) on neuronal activity (Qiu et al., 2016). Finally, parameter I_0 controls the basal neuronal activity in the population, which could stem from synaptic noise or afferent inputs. Table 1 give the full list of model parameters.

Parameter inference

We used Approximate Bayesian Computation (ABC) based on sequential Monte Carlo (SMC) (Toni et al., 2009) to infer four key model parameters (Dyn signalling strength, k_D; NKB signalling strength, k_N; network excitability k_v; and basal activity, I_0) in the estrous and diestrous phase of the ovarian cycle. For this inference we used the average LH pulse frequency observed in four different settings: estrous animals without optic stimulation (F_E) and with 5Hz optic stimulation (F_{E+5Hz}); diestrus animals without optic stimulation (F_D) and with 5Hz optic stimulation (F_{D+5Hz}). Model simulations were generated in Matlab using function ode45 under the four different settings for 6000min and by calculating the frequencies after discarding the initial 1000min. The following discrepancy function was used to compare simulated, $D^* = (F_E^*, F_{E+5Hz}^*, F_D^*, F_{D+5Hz}^*)$, and experimental, $D = (F_E, F_{E+5Hz}, F_D, F_{D+5z})$, data:

$$d(D, D^*) = \max(\mathrm{abs}(D - D^*))$$

Furthermore, for the ABC SMC algorithm the size of the particle population was set to 500 and the algorithm was run for $T = 4$ populations with corresponding tolerance levels $\varepsilon_i = 10^{2-i}, i = 1, \ldots, T$. Prior distributions were formulated in the logarithmic space to explore the behavior of the model under a wide range of parameter values: $\log_{10}(k_D) \sim Uniform(-3,3)$, $\log_{10}(k_N) \sim Uniform(-3,3)$, $\log_{10}(k_v) \sim Uniform(-3,3)$., $\log_{10}(I_0) \sim Uniform(-3,3)$. All remaining parameters were fixed to values found in the literature (see Table 1). For each parameter an independent $\log_{10}$-normal perturbation kernel with variance 0.05 was used.

No	Parameter	Description	Value	Ref.
1	d_D	Dyn degradation rate	0.25 min^{-1}	(Voliotis et al., 2019)
2	d_N	NKB degradation rate	0.25 min^{-1}	(Voliotis et al., 2019)
3	d_v	Firing rate reset rate	10 min^{-1}	(Qiu et al., 2016)
4	k_D	Dyn singalling strength	inferred	
5	k_N	NKB signalling strength	inferred	(Ruka et al., 2016)
6	k_v	Network excitability	inferred	
7	v_0	Maximum rate of neuronal activity increase	30000 spikes min^{-2}	(Qiu et al., 2016)
8	K_D	Dyn IC_{50}	0.3 nM	(Yasuda et al., 1993)

9	K_N	NKB EC_{50}	32 nM	(Seabrook et al., 1995)
10	$K_{v,1}$	Firing rate for half-maximal Dyn secretion	1200 spikes min^{-1}	(Dutton and Dyball, 1979)
11	$K_{v,2}$	Firing rate for half-maximal NKB secretion	1200 spikes min^{-1}	(Dutton and Dyball, 1979)
12	I_0	Basal activity	inferred	
13	n_1, n_2, n_3, n_4	Hill coeffcients	2 (dimensionless)	fixed

Table 1. **Model parameters values**

Sensitivity & Principal Component Analysis

We used principal component analysis to study the sensitivity of the system with respect to changes in the four inferred parameters (Toni et al., 2009). We calculate the principal components in the dataset (sampled posterior distribution) of the inferred parameter changes. Principal component analysis produces a set of linearly uncorrelated eigen-parameters explaining the variance of the inferred changes (in the sampled posterior distribution.) These eigen-parameters are linear weighted combinations of the initial parameters. The eigen-parameter explaining the least of the variance in the posterior distribution corresponds to the stiffest parameter combination. That is small deviations from the inferred way these parameters co-vary would lead to changes in the model behaviour that make it incompatible with the data.

Results

The dynamic response of the KNDy network to sustained, low-frequency optic stimulation is estrous cycle dependent.

Using optogenetics we perturbed the KNDy network to test whether and how sex steroids modulate the system's dynamical response. ARC kisspeptin-expressing neurons were transduced with a Cre-dependent adeno-associated virus (AAV9-EF1-dflox-hChR2-(H134R)-mCherryWPRE-hGH) to express ChR2 (Fig. 1; see Materials and Methods) and were optogenetically stimulated at the estrous and the diestrous phase of the cycle, measuring LH pulse frequency as a readout. Sustained, low-frequency optic stimulation was used to emulate elevated basal activity in ARC kisspeptin neurons or persistent stimulatory signals to the KNDy population from other neuronal populations.

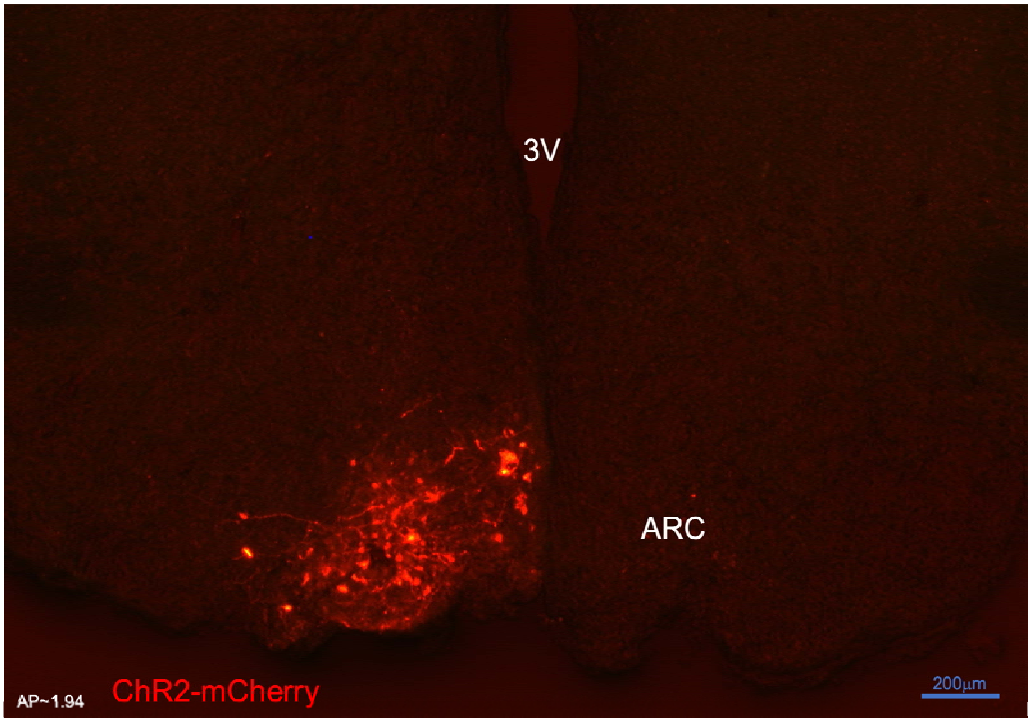

Figure 1. **Expression of arcuate nucleus (ARC) kisspeptin neurones with ChR2-mCherry in Kiss-Cre mouse.** Coronal section showing red mCherry fluorescence positive neurons in the ARC which indicates ChR2 receptor expressing kisspeptin neurones, following unilateral injection of AAV9.EF1.dflox.hChR2(H134R)-mCherry.WPRE.hGH into the ARC of Kiss-Cre mouse. Note the absence of mCherry fluorescence in the other side of ARC. 3V, Third ventricle.

In estrous mice, we find that sustained optogenetic stimulation of ARC kisspeptin neurons at 5Hz immediately triggers robust LH pulses at a frequency of 2.10 ± 0.24 pulses/hour (Fig. 2 A,C&E), which is in agreement with our previous findings (Voliotis et al., 2019) and highlights how pulsatile dynamics can emerge as a population phenomenon without the need of a pulsatile activation signal (Strogatz, 2018). In diestrous mice, on the other hand, optogenetic stimulation of ARC kisspeptin neurons at 5Hz leads to an apparent slowdown of LH pulse frequency towards the end of the 1.5 h stimulation period (SI; Fig. S2). To investigate the response in diestrous mice in greater detail we revised our experimental protocol, removing the control period and extending the stimulation period to 2.5 h. With the extended protocol we measure 0.64 ± 0.09 and 0.40 ± 0.13 LH pulses/hour under sustained optic stimulation at 5 and 15Hz, respectively; these frequencies are significantly lower than the LH pulse frequency we observe in control animals, which receive no optic stimulation (Fig. 2 B,D&F). We note that we observe normal LH pulse frequencies in WT animals receiving sustained optic stimulation for 2.5h (see SI; Fig. S1).

Our data illustrate how natural variation of ovarian steroids across the ovarian cycle leads to qualitative changes in the dynamical response of ARC kisspeptin neurons to optical stimulation. These changes are most probably driven by the effect that gonadal steroids have on the intrinsic electrophysiological properties of ARC kisspeptin neurons (Ruka et al., 2016) and the neuromodulator signalling capacity within the KNDy network (Vanacker et al., 2017).

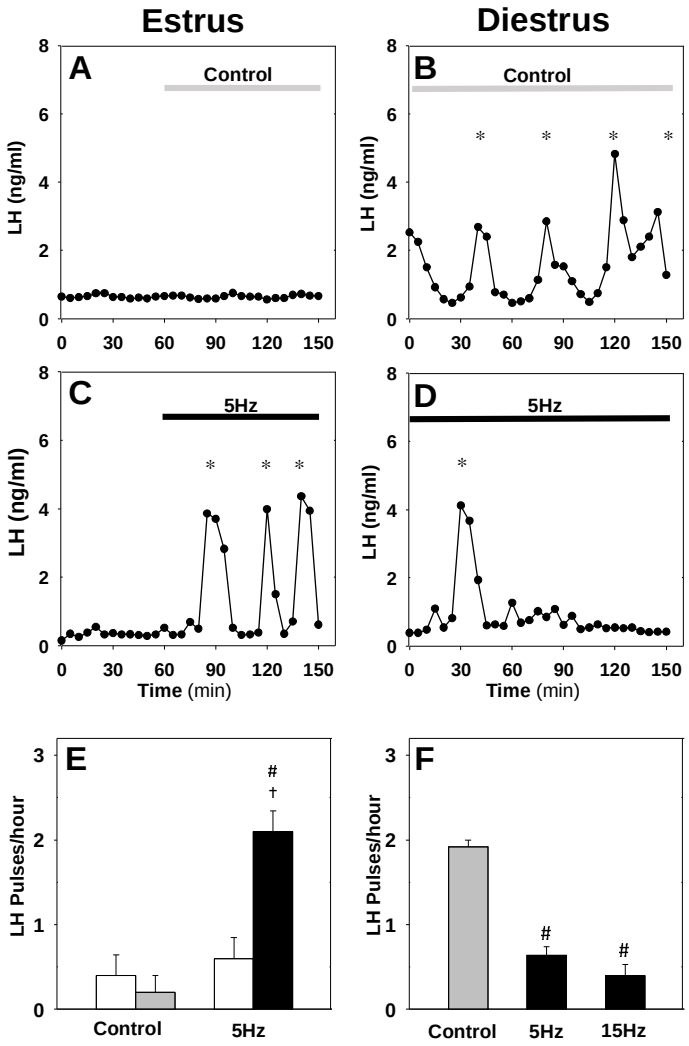

Figure 2. Differential effect of optic stimulation of ARC kisspeptin neurons in estrous and diestrous Kiss-Cre mice. (A-B) Representative examples showing LH secretion in response to no stimulation (grey bar) or sustained blue light (473 nm, 5-ms pulse width, black bar) activation of kisspeptin neurons at 5 Hz in estrous (C) and diestrous (D) mice. (E) Summary showing mean ± SEM LH pulse frequency over the 60min control period (white bars) and over the subsequent stimulation period (black bar) in estrous mice. (F) Summary showing mean ± SEM LH pulse frequency in the control (grey bar) and stimulated (black bars) diestrous mice. *Denote LH pulses. $^{\#}P < 0.05$ vs control; $^{\dagger}P < 0.05$ vs pre-stimulation; n = 5-6 per group.

A mathematical model predicts key mechanisms modulating the behaviour of the KNDy pulse generator across the estrous cycle.

Interrogating the KNDy network at different stages of the estous cycle via optic stimulation and measuring the effect on LH pulse frequency allows use of our mathematical model (Voliotis et al., 2019) to understand how key system parameters change under gonadal steroid control. The model describes the dynamical behaviour of ARC kisspeptin neurons using three dynamical variables: representing the levels of Dyn, NKB and neuronal activity (Fig. 3 A). We postulate that gonadal steroids could potentially modulate the behaviour of the KNDy system across the cycle via acting on four key model parameters: (i) level of Dyn signalling, (ii) level of NKB signalling, (iii) network excitability (i.e., propensity of neurons in the population to transmit signals to one another), and (iv) basal neuronal activity.

Employing Bayesian inference techniques (see material and methods), we sample values for these four parameters, which allow the model to replicate the mean LH frequency we observe experimentally in estrus and diestrus mice with and without 5Hz optic stimulation (Fig. 2 E&F). Inspection of the dynamical behaviour of the model, using the identified diestrous parameter values, reveals that in response to optic stimulation in diestrus pulsatile dynamics could die out gradually (i.e, there is a transient period before activity shuts down; see Fig. 3 B for an illustrative example), which is confirmed by the delayed inhibition of LH pulses we observed experimentally in diestrous mice.

Next, we focus on how the four key parameters change between diestrus and estrus. We measure the change in each parameter using the log-ratio of its estrous to diestrous value, and calculate the covariance matrix of these log-ratios from our set of inferred parameter values. We find a positive (linear) correlation between changes in Dyn and NKB signalling strength, and negative (linear) correlation between changes in NKB signalling strength and network excitability (Fig. 3 C). That is, the model predicts that NKB signalling strength and network excitability are characterised by opposite (in direction) correlations during the transition from diestrus to estrus (one decreasing the other increasing; we note the model predicts that both combinations are possible), whereas NKB and Dyn signalling remain correlated in the same direction (ether increasing or decreasing; we note the model predicts that both combinations are possible). Finally, we apply Principal Component Analysis to study the sensitivity of the system with respect to changes in the four parameters (see Materials and Methods). We calculate the principal components in dataset with the inferred parameter changes. Principal components explaining small portions of the variance in the dataset (i.e., principal component

with the smallest eigenvalue) correspond to parameter combinations to which the system dynamics are most sensitive (stiff parameter combinations). These combinations are the most critical in terms of regulation as small deviations in how these parameters co-vary result in significant shifts in the system's dynamics. Interestingly, the principal component capturing the smallest share of the variance is comprised of the parameters controlling NKB signalling, Dyn signalling and network excitability in approximately equal portions, and therefore the model predicts that co-ordinated changes in these three parameters should be critical for the observed changes in system dynamics between diestrus and estrus. Interestingly, the second smallest principal component is largely determined by change in the basal activity parameter, suggesting that basal activity is another independent handle for modulating the system's dynamics. Taken together our theoretical findings suggest that co-ordinated changes in KNDy signalling as well as changes in KNDy basal activity may be crucial pathways of regulation across the reproductive cycle.

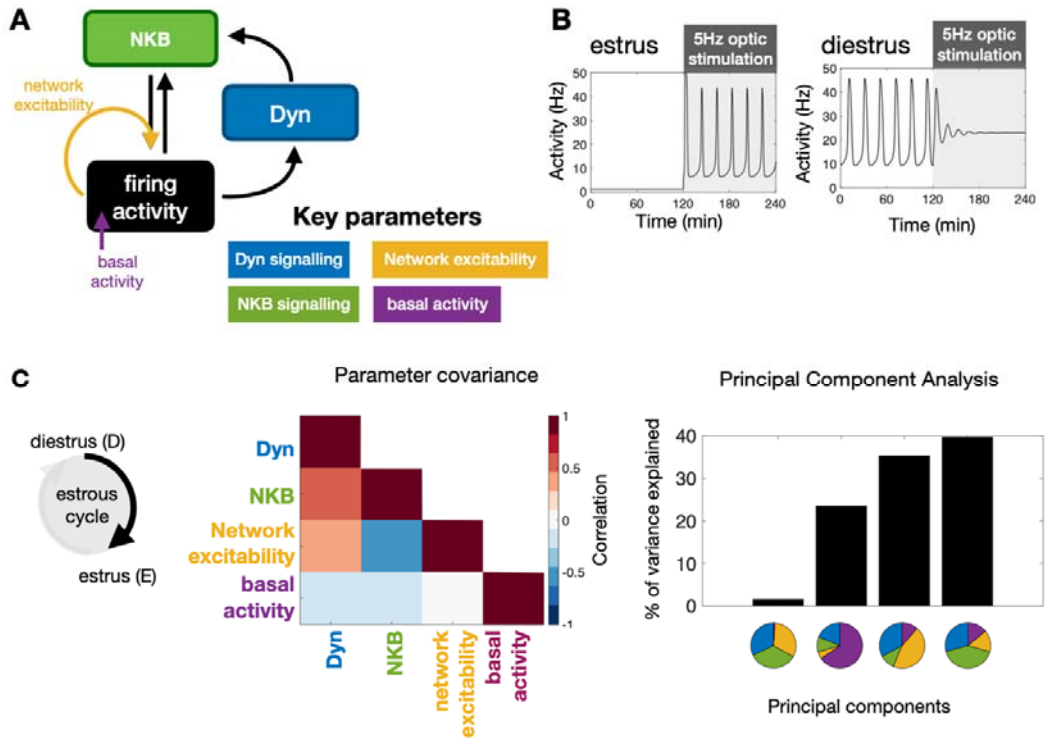

Figure 3. Model predictions on the key mechanisms modulating the behaviour of the KNDy pulse generator across the ovarian cycle. (A) Schematic illustration of the coarse-grained model of the ARC KNDy population. The model comprises three dynamical variables representing the average levels of Dyn and NKB secreted by the population, and its average firing activity. We hypothesise that four key parameters modulate the behaviour of the system across the ovarian cycle: (i) Dyn signalling strength; (ii) NKB signalling strength; (iii) network excitability and (iv) basal neuronal activity. Estimates for the four parameters in estrus and diestrus are

inferred from LH pulse frequency data in estrus and diestrus animals; with or without 5Hz optic stimulation (Fig. 2 E&F) (B) System response to low frequency stimulation during estrus and diestrus, using the maximum a-posteriori estimate of the parameter values inferred from the frequency data. (C) Analysis of parameter changes across the cycle. For each of the four parameter (θ^i; $i = 1,2,3,4$) the diestrus-to-estrus change is defined as the log-ratio between the corresponding parameter values, i.e., $\log_{10} \theta^i_{\text{estrus}} / \theta^i_{\text{diestrus}}$. Normalised covariance (correlation) matrix of parameter changes reveals negative correlation between changes in NKB signalling strength and network excitability, and positive correlation between Dyn signalling strength and both NKB signalling. Eigen-parameters are visualised as pie charts. The eigen-parameter explaining the least of the variance in the posterior distribution corresponds to the stiffest parameter combination to which the system is most sensitive.

Glutamatergic transmission in the KNDy population is critical for LH pulsatility

Since KNDy neurons are primarily glutamatergic (Cravo et al., 2011; Nestor et al., 2016; Qiu et al., 2016; Qiu et al., 2018) and synapse to one another (Yip et al., 2015; Qiu et al., 2016) we hypothesise that glutamate transmission is a key driver of excitability within the KNDy network. Hence to better understand how network excitability affects the dynamic behaviour of the system across the ovarian cycle as the model predicts we disrupt signalling via glutamate receptors and quantify the impact of this disruption on LH pulsatility.

First, using Kiss-Cre estrous mice we test whether glutamatergic transmission is necessary for the optogenetic induction of LH pulses. We drive the ARC kisspeptin population using sustained, low-frequency optic stimulation (5 Hz) in the presence of the combined NMDA and AMPA receptor antagonists (AP5 and CNQX, respectively). We find that blocking signalling via glutamate receptors inhibits the capacity of optic stimulation to generate and sustain pulsatile LH secretion (Fig. 4 A,B&D). The combined AP5 and CNQX in the absence of optic stimulation had no effect (Fig. 4 C&D).

Next, we test whether glutamatergic transmission is critical for the endogenous LH pulses observed in diestrus. Treatment of diestrous mice with the combined NMDA and AMPA receptor antagonists resulted in a significant reduction of LH pulse frequency from 2.50 ± 0.29 to 0.45 ± 0.15 pulses/hour (Fig. 5 B&D), confirming that the glutamatergic transmission is indeed critical for pulsatility. Moreover, combining NMDA and AMPA receptor antagonist treatment with low frequency optic stimulation (5 Hz) partially restored LH pulsatility to 1.58 ± 0.17 pulses/hour (Fig. 5 C&D), suggesting low glutamatergic transmission within the KNDy population or from upstream neuronal populations could be offset by other exogenous inputs or elevated basal activity. This finding is in agreement with the model prediction that

basal activity and signalling between KNDy neurons are independent pathways of modulating the system's dynamical behaviour.

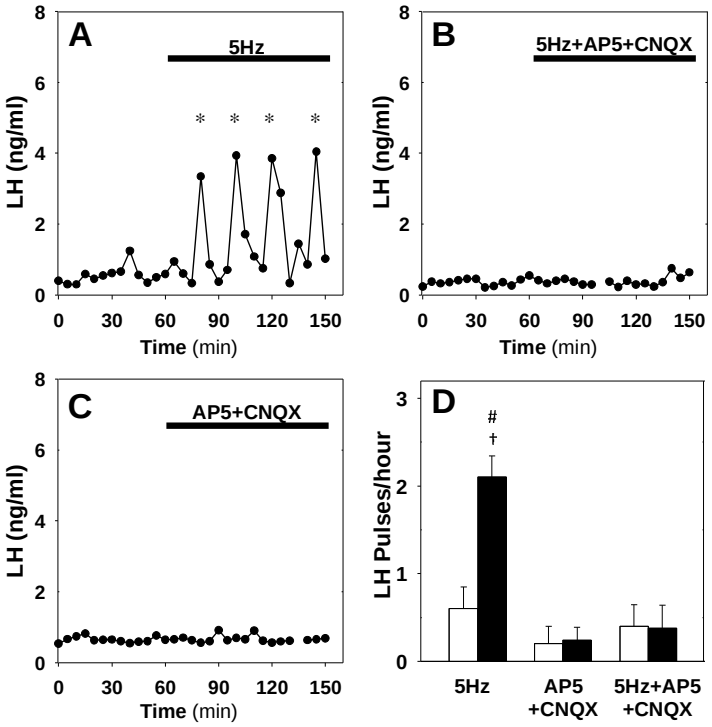

Figure 4. Effect of NMDA+AMPA receptor antagonists on pulsatile LH secretion in estrus. Representative examples showing LH secretion in estrous mice in response to optic stimulation (5Hz blue light, 473 nm, 5-ms pulse width) (A) and optic stimulation combined with the NMDA+AMPA receptor antagonist (bolus ICV injection [12 nmol AP5 + 5 nmol CNQX] over 5 min, followed by a continuous infusion [20 nmol AP5 and 10 nmol CNQX] for the remaining 90 min) treatment (B). NMDA+AMPA receptor antagonist alone had no effect (C). (D) Summary showing mean ± SEM LH pulse frequency over the 60min non-stimulatory period (white bars) and over the subsequent 90 min stimulation period or appropriate non-stimulatory period in presence of. NMDA+AMPA receptor antagonist alone (black bar) in diestrous mice. *Denote LH pulses. $^{\dagger}P < 0.05$ vs pre-stimulation. $^{\#}P < 0.05$ compared to antagonist treatment groups; n = 5-6 per group.

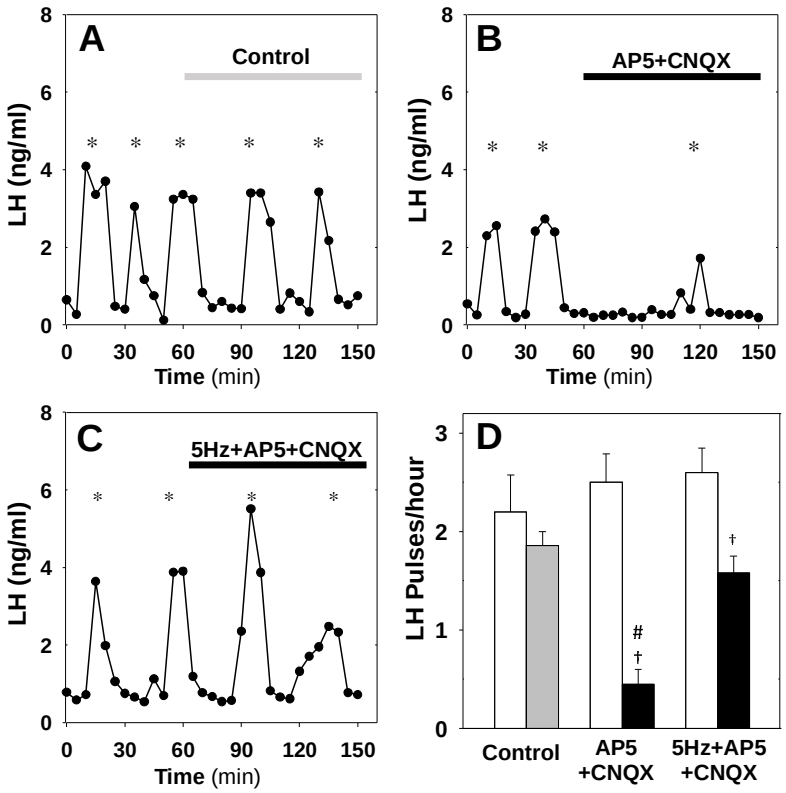

Figure 5. Effect of NMDA+AMPA receptor antagonists on pulsatile LH secretion in diestrus. Representative examples showing pulsatile LH secretion in response to ICV administration of aCSF as control (A), treatment with NMDA+AMPA receptor antagonists (AP5+CNQX: bolus ICV injection [12 nmol AP5 + 5 nmol CNQX] over 5 min, followed by a continuous infusion [20 nmol AP5 and 10 nmol CNQX] for the remaining 90 min) (B) and combined NMDA/AMPA receptor antagonist treatment and sustained optic stimulation (blue light 473 nm, 5-ms pulse width) at 5Hz (C). (D) Summary showing mean ± SEM LH pulse frequency over the 60min non-stimulatory period (white bars) and over the subsequent 90 min stimulation period in control mice (grey bar) and mice receiving treatment (black bar). *Denote LH pulses. $^{\dagger}P < 0.05$ vs pre-stimulation. $^{\#}P < 0.05$ compared to 5 Hz stimulation plus antagonist treatment and aCSF control groups; n = 5-6 per group.

Discussion

Using optogenetics we perturbed the GnRH pulse generator at different stages of the ovarian cycle aiming to understand how gonadal steroids modulate key properties of the system. Previous studies have shown how the pulsatile activity generated by the kisspeptin neuronal network is modulated across the estrous cycle (Han et al., 2015; McQuillan et al., 2019). Our data show that the stage of the cycle also has a profound effect on the dynamical response of the kisspeptin population to sustained, low frequency optic stimulation. Such stimulation

triggers acceleration of LH pulses during estrus and deaccelarion during diestrus. Previously, our mathematical model of the KNDy network has predicted an upper and a lower bifurcation point that determine the system's range of pulsatile behaviour as the system is driven externally (Voliotis et al., 2019). Our data suggest that the gonadal state plays a critical role in shifting these bifurcation points by modulating key parameters of the system. In particular, during estrous the system is positioned below the lower bifurcation point and optogenetic stimulation of ARC kisspeptin neurons at 5Hz move the system across the lower bifurcation point leading to the sudden emergence of pulsatile behaviour. In contrast, during diestrus the system is within the pulsatile regime and optogenetic stimulation of ARC kisspeptin neurons at frequencies greater than 5Hz move the system across the upper bifurcation point and its dynamics relax progressively from pulsatile to quiescent. Our data therefore highlight the critical role of gonadal steroids in modulating the dynamical response of the KNDy network to small changes in basal activity of ARC kisspeptin neurons or in how the population processes external perturbations and afferent inputs.

Using our mathematical model of the system we gained insight into possible mechanisms via which gonadal steroids modulate the dynamic behaviour of the GnRH pulse generator. Based on the LH pulse frequency observed in estrous and diestrous animals under no optic stimulation or with 5Hz optic stimulations, the model predicted that network excitability is an important parameter of the system, which could be modulated at different stages of the ovarian cycle. Importantly, KNDy network excitability is most probably co-regulated with parameters controlling the strength of Dyn and NKB signalling as the system transitions between the different phases of the ovarian cycle. In particular, our analysis suggests strong negative correlation between changes in NKB signalling strength and changes in network excitability and strong positive correlation in changes between NKB and Dyn signalling. Interestingly these finding are in line with recent transcriptomic data showing that treatment of ovariectomised mice with estradiol reduced expression of NKB and Dyn in KNDy neurons, but increased expression of glutamate transporters (vGlut2), which lead to increased glutamate neurotransmission and neuronal excitability in the population (Qiu et al., 2018).

The effect of cycle stage on the LH response to sustained optogenetic stimulation is reminiscent of the well documented effect that gonadal steroids have on LH response to various excitatory neurotransmitters and neuropeptides (e.g., NMDA). For instance, investigations in the female monkey revealed an unexplained inhibition of LH in OVX

animals following treatment with NMDA, in contrast with the excitatory action of NMDA on LH secretion in the presence of ovarian steroids (Reyes et al., 1990; Reyes et al., 1991). Similar reversal of action on LH dynamics depending on the underlying ovarian steroid milieu has been documented for various other neurotransmitters and NKB receptor agonists (Kalra and Kalra, 1983; Scorticati et al., 2004). Our mathematical model supports that ovarian steroids change key parameters of the KNDy network, which control the dynamic behaviour of the system and its response to perturbations. As an illustration, Fig. 6 shows how the dynamic behaviour of the model depends on network excitability and NKB signalling. Since these parameters are governed by gonadal steroids (Qiu et al., 2018; Wang et al., 2018), it is expected that the underlying steroid milieu will also modulate the effect of perturbations on the dynamics of the system. For instance, the effect of stimulating NKB signalling (e.g., via administration of NK3 receptor agonists) or network excitability (e.g., via NMDA administration) could result in inhibition of the pulse generator if the system is already located closer to the right boundary of the pulsatile dynamics region (e.g., point B in Fig. 6). Such points correspond to states with high pulse generator activity similar to pulse generator dynamics observed in many animal models after gonadectomy (Reyes et al., 1990; Kinsey-Jones et al., 2012). In contrast, similar perturbations but from a different point in the parameter space, lying closer to the left edge of the pulsatile region (e.g., point A in Fig. 6), could result in stimulation of the pulse generator (higher frequency). This illustrative example also highlights that the effect of gonadal steroids on the response of the pulse generator to perturbations is continuous rather than binary, that is, the behaviour of the pulse generator is modulated by the actual continuous levels of gonadal steroids rather than their mere presence of absence. Therefore, the underlying steroid levels could explain seemingly incompatible findings regarding the effect of NKB receptor agonism on LH secretion: ranging from stimulation (Navarro et al., 2011) or inhibition (Sandoval-Guzman and Rance, 2004; Kinsey-Jones et al., 2012) to no effects (Navarro et al., 2009) in rodents.

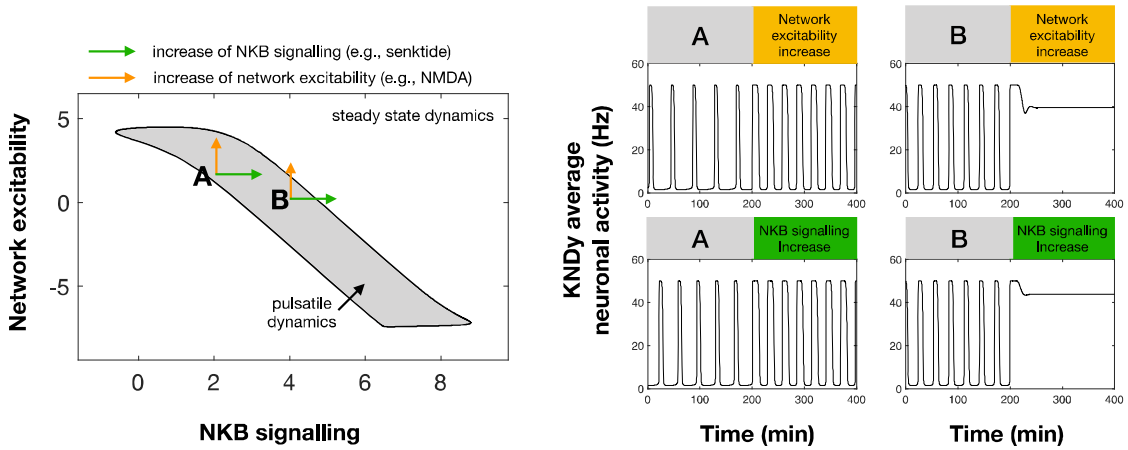

Figure 6. Differential effect of perturbations on the dynamics of the pulse generator. Two-parameter (NKB signalling and Network excit ability) bifurcation diagram showing the region in the parameter space for which the system exhibits pulsatile dynamics (grey area). Two points (denoted by A and B) illustrate how an increase in NKB signalling or network excitability could have a differential effect on the dynamics of the system. For point A an increase in network excitability or NKB signalling could lead to an increase in the frequency and width of pulses. However, for point B a similar increase leads to pulse inhibition and steady state system dynamics.

Based on our model predictions regarding the importance of network excitability, we set out to uncover the role of this parameter on the dynamic response of the network in-vivo. We hypothesised that network excitability should critically depend on the levels of glutamate signalling as ARC kisspeptin neurons are known to be interconnected (Yip et al., 2015; Qiu et al., 2016) and communicate via glutamate (Cravo et al., 2011; Qiu et al., 2011; Nestor et al., 2016; Qiu et al., 2016). Further evidence that estradiol regulates KNDy neuronal excitability (Qiu et al., 2018) and that cycle stage regulates spontaneous glutamatergic activity of KNDy neurons (Wang and Moenter, 2020) supports the model prediction that network excitability is a critical network property regulated by gonadal steroids. Therefore, to further test this prediction in-vivo we used glutamate receptor (NMDA and AMPA) antagonists to inhibit excitability in the KNDy network. In diestrus animals blocking glutamate receptors (NMDA and AMPA) inhibited LH pulses that were then rescued via low frequency optogenetic stimulation of kisspeptin neurons. Furthermore, in estrus animals, NMDA and AMPA receptor antagonism inhibited the induction of LH pulses via optic stimulation. These experimental findings highlight the complex fine-balanced mechanisms underlying pulse generation by the KNDy network. In particular, limited glutamatergic signalling within the KNDy population blocks LH pulsatility but this can be mitigated by elevated basal neuronal activity. Similarly, increased basal neuronal activity can induce pulse generation but this effect can be negated by decreased glutamatergic signalling within the neuronal population. . There is a caveat, however, as the glutamate receptor antagonists were given by intracerebroventricular injection and this raises the possibility of additionally

interfering with glutamatergic transmission from afferent populations. However, to the best of our knowledge there is no clear evidence of such glutamatergic inputs into the KNDy population. Furthermore, blocking possible exogenous glutamatergic inputs does not invalidate our model, but further supports one of its key predictions that basal activation of KNDy neurons is a critical pathway for modulating the dynamics of the pulse generator. Overall, our model predicts that pulse generation is an emergent property of the KNDy network depending both on single neuron properties such as basal activity and exogeneous activation but also on how the neurons signal and communicate with each other. Our results support this idea, highlighting the critical role of glutamate in enabling the population to pulse in synchrony.

Acknowledgments: The authors gratefully acknowledge the financial support of the EPSRC via grant EP/N014391/1 (KTA and MV), and BBSRC via grants BB/S000550/1 and BB/S001255/1 (KTA, KOB, MV, XFL).

References

Arias P, Jarry H, Leonhardt S, Moguilevsky JA, Wuttke W (1993) Estradiol modulates the LH release response to N-methyl-D-aspartate in adult female rats: studies on hypothalamic luteinizing hormone-releasing hormone and neurotransmitter release. Neuroendocrinology 57:710-715.

Bonavera JJ, Sahu A, Kalra SP, Kalra PS (1994) The hypothalamic peptides, beta-endorphin, neuropeptide K and interleukin-1 beta, and the opiate morphine, enhance the excitatory amino acid-induced LH release under the influence of gonadal steroids. J Neuroendocrinol 6:557-564.

Brann DW, Mahesh VB (1992) Excitatory amino acid regulation of gonadotropin secretion: modulation by steroid hormones. J Steroid Biochem Mol Biol 41:847-850.

Christian CA, Moenter SM (2010) The neurobiology of preovulatory and estradiol-induced gonadotropin-releasing hormone surges. Endocr Rev 31:544-577.

Cravo RM, Margatho LO, Osborne-Lawrence S, Donato J, Jr., Atkin S, Bookout AL, Rovinsky S, Frazao R, Lee CE, Gautron L, Zigman JM, Elias CF (2011) Characterization of Kiss1 neurons using transgenic mouse models. Neuroscience 173:37-56.

Czieselsky K, Prescott M, Porteous R, Campos P, Clarkson J, Steyn FJ, Campbell RE, Herbison AE (2016) Pulse and Surge Profiles of Luteinizing Hormone Secretion in the Mouse. Endocrinology 157:4794-4802.

Dutton A, Dyball RE (1979) Phasic firing enhances vasopressin release from the rat neurohypophysis. J Physiol 290:433-440.

Goodman RL, Holaskova I, Nestor CC, Connors JM, Billings HJ, Valent M, Lehman MN, Hileman SM (2011) Evidence that the arcuate nucleus is an important site of progesterone negative feedback in the ewe. Endocrinology 152:3451-3460.

Han SY, McLennan T, Czieselsky K, Herbison AE (2015) Selective optogenetic activation of arcuate kisspeptin neurons generates pulsatile luteinizing hormone secretion. Proc Natl Acad Sci U S A 112:13109-13114.

Kalra SP, Kalra PS (1983) Neural regulation of luteinizing hormone secretion in the rat. Endocr Rev 4:311-351.

Kelly MJ, Zhang C, Qiu J, Ronnekleiv OK (2013) Pacemaking kisspeptin neurons. Exp Physiol 98:1535-1543.

Kinsey-Jones JS, Grachev P, Li XF, Lin YS, Milligan SR, Lightman SL, O'Byrne KT (2012) The inhibitory effects of neurokinin B on GnRH pulse generator frequency in the female rat. Endocrinology 153:307-315.

Lass G, Li XF, de Burgh RA, He W, Kang Y, Hwa-Yeo S, Sinnett-Smith LC, Manchishi SM, Colledge WH, Lightman SL, O'Byrne KT (2020) Optogenetic stimulation of kisspeptin neurones within the posterodorsal medial amygdala increases luteinising hormone pulse frequency in female mice. J Neuroendocrinol 32:e12823.

McQuillan HJ, Han SY, Cheong I, Herbison AE (2019) GnRH Pulse Generator Activity Across the Estrous Cycle of Female Mice. Endocrinology 160:1480-1491.

Moore AM, Coolen LM, Porter DT, Goodman RL, Lehman MN (2018) KNDy Cells Revisited. Endocrinology 159:3219-3234.

Navarro VM, Gottsch ML, Chavkin C, Okamura H, Clifton DK, Steiner RA (2009) Regulation of gonadotropin-releasing hormone secretion by kisspeptin/dynorphin/neurokinin B neurons in the arcuate nucleus of the mouse. J Neurosci 29:11859-11866.

Navarro VM, Castellano JM, McConkey SM, Pineda R, Ruiz-Pino F, Pinilla L, Clifton DK, Tena-Sempere M, Steiner RA (2011) Interactions between kisspeptin and neurokinin B in the control of GnRH secretion in the female rat. Am J Physiol Endocrinol Metab 300:E202-210.

Nestor CC, Qiu J, Padilla SL, Zhang C, Bosch MA, Fan W, Aicher SA, Palmiter RD, Ronnekleiv OK, Kelly MJ (2016) Optogenetic Stimulation of Arcuate Nucleus Kiss1 Neurons Reveals a Steroid-Dependent Glutamatergic Input to POMC and AgRP Neurons in Male Mice. Mol Endocrinol 30:630-644.

Paxinos G, Franklin KBJ (2004) The Mouse Brain in Stereotaxic Coordinates, 2nd Edition: Elsevier Academic Press.

Qiu J, Fang Y, Bosch MA, Ronnekleiv OK, Kelly MJ (2011) Guinea pig kisspeptin neurons are depolarized by leptin via activation of TRPC channels. Endocrinology 152:1503-1514.

Qiu J, Nestor CC, Zhang C, Padilla SL, Palmiter RD, Kelly MJ, Ronnekleiv OK (2016) High-frequency stimulation-induced peptide release synchronizes arcuate kisspeptin neurons and excites GnRH neurons. Elife 5:e16246-e16246.

Qiu J, Rivera HM, Bosch MA, Padilla SL, Stincic TL, Palmiter RD, Kelly MJ, Ronnekleiv OK (2018) Estrogenic-dependent glutamatergic neurotransmission from kisspeptin neurons governs feeding circuits in females. Elife 7.

Reyes A, Luckhaus J, Ferin M (1990) Unexpected inhibitory action of N-methyl-D,L-aspartate or luteinizing hormone release in adult ovariectomized rhesus monkeys: a role of the hypothalamic-adrenal axis. Endocrinology 127:724-729.

Reyes A, Xia LN, Ferin M (1991) Modulation of the effects of N-methyl-D,L-aspartate on luteinizing hormone by the ovarian steroids in the adult rhesus monkey. Neuroendocrinology 54:405-411.

Ruka KA, Burger LL, Moenter SM (2016) Both Estrogen and Androgen Modify the Response to Activation of Neurokinin-3 and kappa-Opioid Receptors in Arcuate Kisspeptin Neurons From Male Mice. Endocrinology 157:752-763.

Sandoval-Guzman T, Rance NE (2004) Central injection of senktide, an NK3 receptor agonist, or neuropeptide Y inhibits LH secretion and induces different patterns of Fos expression in the rat hypothalamus. Brain Res 1026:307-312.

Scorticati C, Fernandez-Solari J, De Laurentiis A, Mohn C, Prestifilippo JP, Lasaga M, Seilicovich A, Billi S, Franchi A, McCann SM, Rettori V (2004) The inhibitory effect of anandamide on luteinizing hormone-releasing hormone secretion is reversed by estrogen. Proc Natl Acad Sci U S A 101:11891-11896.

Seabrook GR, Bowery BJ, Hill RG (1995) Pharmacology of tachykinin receptors on neurones in the ventral tegmental area of rat brain slices. Eur J Pharmacol 273:113-119.

Steyn FJ, Wan Y, Clarkson J, Veldhuis JD, Herbison AE, Chen C (2013) Development of a methodology for and assessment of pulsatile luteinizing hormone secretion in juvenile and adult male mice. Endocrinology 154:4939-4945.

Strogatz SH (2018) Nonlinear dynamics and chaos with student solutions manual: With applications to physics, biology, chemistry, and engineering: CRC press.

Toni T, Welch D, Strelkowa N, Ipsen A, Stumpf MP (2009) Approximate Bayesian computation scheme for parameter inference and model selection in dynamical systems. J R Soc Interface 6:187-202.

Vanacker C, Moya MR, DeFazio RA, Johnson ML, Moenter SM (2017) Long-Term Recordings of Arcuate Nucleus Kisspeptin Neurons Reveal Patterned Activity That Is Modulated by Gonadal Steroids in Male Mice. Endocrinology 158:3553-3564.

Vidal A, Zhang Q, Medigue C, Fabre S, Clement F (2012) DynPeak: an algorithm for pulse detection and frequency analysis in hormonal time series. PLoS One 7:e39001.

Voliotis M, Li XF, De Burgh R, Lass G, Lightman SL, O'Byrne KT, Tsaneva-Atanasova K (2019) The Origin of GnRH Pulse Generation: An Integrative Mathematical-Experimental Approach. J Neurosci 39:9738-9747.

Wang L, Moenter SM (2020) Differential Roles of Hypothalamic AVPV and Arcuate Kisspeptin Neurons in Estradiol Feedback Regulation of Female Reproduction. Neuroendocrinology 110:172-184.

Wang L, Burger LL, Greenwald-Yarnell ML, Myers MG, Jr., Moenter SM (2018) Glutamatergic Transmission to Hypothalamic Kisspeptin Neurons Is Differentially Regulated by Estradiol through Estrogen Receptor alpha in Adult Female Mice. J Neurosci 38:1061-1072.

Yasuda K, Raynor K, Kong H, Breder CD, Takeda J, Reisine T, Bell GI (1993) Cloning and functional comparison of kappa and delta opioid receptors from mouse brain. Proc Natl Acad Sci U S A 90:6736-6740.

Yeo SH, Kyle V, Morris PG, Jackman S, Sinnett-Smith LC, Schacker M, Chen C, Colledge WH (2016) Visualisation of Kiss1 Neurone Distribution Using a Kiss1-CRE Transgenic Mouse. J Neuroendocrinol 28.

Yip SH, Boehm U, Herbison AE, Campbell RE (2015) Conditional Viral Tract Tracing Delineates the Projections of the Distinct Kisspeptin Neuron Populations to Gonadotropin-Releasing Hormone (GnRH) Neurons in the Mouse. Endocrinology 156:2582-2594.